Eur Radiol (2007) 17: 1634–1643
DOI 10.1007/s00330-006-0459-z

Andreas Gartus
Alexander Geissler
Thomas Foki
Amir Reza Tahamtan
Gerald Pahs
Markus Barth
Katja Pinker
Siegfried Trattnig
Roland Beisteiner

Comparison of fMRI coregistration results between human experts and software solutions in patients and healthy subjects

Received: 21 March 2006
Revised: 22 June 2006
Accepted: 25 August 2006
Published online: 12 October 2006

A. Gartus · A. Geissler · T. Foki · A. R. Tahamtan · G. Pahs · M. Barth · K. Pinker · S. Trattnig · R. Beisteiner (✉)
Study Group Clinical fMRI at the Departments of Neurology, Neurosurgery and Radiology, MR Center of Excellence, Medical University of Vienna, Waehringer Guertel 18-20, 1090 Vienna, Austria
e-mail: roland.beisteiner@meduniwien.ac.at
Tel.: +43-1-404003117
Fax: +43-1-404003141

A. Gartus · A. Geissler · T. Foki · A. R. Tahamtan · G. Pahs · R. Beisteiner
Ludwig Boltzmann Institute for Functional Brain Topography, Medical University of Vienna, Waehringer Guertel 18-20, 1090 Vienna, Austria

A. Gartus · A. Geissler · T. Foki · A. R. Tahamtan · G. Pahs · R. Beisteiner
Department of Neurology, Medical University of Vienna, Waehringer Guertel 18-20, 1090 Vienna, Austria

M. Barth · K. Pinker · S. Trattnig
Department of Radiology, Medical University of Vienna, Waehringer Guertel 18-20, 1090 Vienna, Austria

M. Barth
FC Donders Centre for Cognitive Neuroimaging, Radboud University, P.O. Box 9101, 6500 HB Nijmegen, The Netherlands

Abstract Functional magnetic resonance imaging (fMRI) performed by echo-planar imaging (EPI) is often highly distorted, and it is therefore necessary to coregister the functional to undistorted anatomical images, especially for clinical applications. This pilot study provides an evaluation of human and automatic coregistration results in the human motor cortex of normal and pathological brains. Ten healthy right-handed subjects and ten right-handed patients performed simple right hand movements during fMRI. A reference point chosen at a characteristic anatomical location within the fMRI sensorimotor activations was transferred to the high resolution anatomical MRI images by three human fMRI experts and by three automatic coregistration programs. The 3D distance between the median localizations of experts and programs was calculated and compared between patients and healthy subjects. Results show that fMRI localization on anatomical images was better with the experts than software in 70% of the cases and that software performance was worse for patients than healthy subjects (unpaired t-test: P=0.040). With 45.6 mm the maximum disagreement between experts and software was quite large. The inter-rater consistency was better for the fMRI experts compared to the coregistration programs (ANOVA: P=0.003). We conclude that results of automatic coregistration should be evaluated carefully, especially in case of clinical application.

Keywords Functional MRI · 3D linear coregistration · Clinical brain mapping · Healthy subjects · Patients

Introduction

Functional magnetic resonance imaging (fMRI) (compare, e.g., [1, 2]) is used in various ways in clinical practice. Its applications include preoperative mapping of cortical functions to avoid damage of eloquent brain areas during surgery (e.g., [3–5]), postoperative investigation of brain function recovery (e.g., [5, 6]) and evaluation of brain activation in patients suffering from degenerative brain diseases (e.g., [7]). Especially the identification of

brain areas that are essential for language, motor control or memory functions and that therefore must be excluded from resection is crucial for neurosurgical planning and treatment.

The most widely used method for fMRI is echo-planar imaging (EPI) (e.g., [8]). However, EPI is also very sensitive to B0 field inhomogeneities. Furthermore, EPI offers insufficient contrast and resolution for clinical application. Thus, it is necessary to map the distorted functional EPI data on anatomically correct high-resolution MR images, which is a challenging and error-prone procedure. The exact transfer of neuronal activation to the correct corresponding neuroanatomical structure of non-distorted anatomical images is especially difficult in the presence of brain pathology. To utilize the fine localization capability of functional EPI images [9], functional anatomical registration is an absolutely essential procedure—in particular for clinical applications.

Many techniques were proposed to register EPI images with undistorted anatomy. These include direct overlay [10–12], optimized shimming [13–15], special fMRI sequences [16, 17] or recently developed experimental B0 field mapping techniques [18–22]. However, most reports try to improve the quality of the functional overlay by linear [20, 23–27] or non-linear [28–30] coregistration of the distorted EPI images with anatomical images.

While clearly automation of functional-anatomical coregistration is desired, for secure clinical application substantial knowledge about possible localization errors is mandatory. As a first step, this work evaluates the coregistration accuracy of three software packages (SPM2, FSL and vtkCISG) in the human motor cortex, two of them being in widespread experimental and clinical use (SPM2; FSL). The main goal of our study was to find out whether relevant differences may exist between functional localizations performed by three clinical fMRI experts and those performed by three software packages. Results were expected to provide a first hint about clinical functional reliability of widely used software solutions.

Materials and methods

Comparable to related studies [10, 11, 24–26, 31–37], two groups of ten participants each were recruited for this investigation. Healthy right-handed volunteers (three females and seven males; mean age: 23.9 years; standard deviation: 4.3 years) and right-handed patients (six females and four males; mean age: 41.0 years; standard deviation: 16.3 years) suffering from large brain lesions. All subjects gave informed written consent and the study was approved by the local ethics committee.

To generate realistic functional EPI data for image processing, all subjects performed six to seven runs of the simple motor task of self-initiated and self-paced opening and closing of the right hand. Each run consisted of four rest and three movement phases with 20-s duration each. Acoustic commands transmitted via earphones indicated the start and stop of the movement phases to the subjects.

To minimize head motion artifacts, individually constructed plaster cast helmets [38] were used for optimized and secure head fixation. A 3-T (Tesla) BRUKER whole body system with head coil (Medspec 3000, BRUKER Biospin, Ettlingen, Germany; field strength 3 T; receiver bandwidth 167 kHz; read gradient strength 45 mT/m) was used for the fMRI measurements. We applied a phase-corrected single-shot blipped GE-EPI sequence (TE/TR= 55.5/4,000 ms; 128×128 matrix; 230×230-mm field of view (FOV); 25 axial slices; slice thickness 3 mm; voxel size 1.8×1.8×3 mm; no interslice gap; sinc-pulse excitation). All volumes of every subject were realigned using AIR 3.08 [39] (http://bishopw.loni.ucla.edu/AIR3) with a rigid six-parameter (three transformation and three rotation parameters) model prior to further analysis. In four healthy subjects (out of ten) and four patients (out of ten), the realignment procedure led to data loss in bottom slices. In addition, two patients (out of ten) and three healthy subjects (out of ten) showed some data loss in top slices. In all cases only one top and/or bottom slice was affected.

Conventional anatomical MRI data sets (T1-weighted; MDEFT, 256×256 matrix; 230×230-mm FOV; 128 axial slices; slice thickness 1.8 mm; voxel size 0.9×0.9×1.8 mm) covering the whole brain were recorded additionally for overlay with the functional data. In addition, two anatomical patient data sets were also recorded on a 1.5-T Philips system (Philips Medical Systems, Gyroscan Intera).

From each subject the first EPI volume was selected as reference volume for the automatic coregistration process. One of the authors defined a reference point in the functional images within the primarily activated structures of the central sulcus/primary motor cortex at a characteristic location (e.g., a sharp bend of the precentral gyrus, compare Fig. 1). While the gold standard of functional localization would be an electrophysiological technique as, e.g., intraoperative cortical stimulation, this was not used in our work, since we only manually chose a reference point to obtain a localization that can be easily identified in both the functional and the anatomical images.

Subsequently, each reference point was transferred to the corresponding anatomical structure of the high-resolution anatomical MR images by three clinical fMRI experts, each with a professional background in neurology or radiology and long-standing experience with MR image analysis. For this procedure the different resolution of the two data sets needs to be taken into account and a careful analysis of anatomical structures of both functional and anatomical images is necessary (see Fig. 1). The analysis is complex, time consuming and requires specific training, especially for evaluation of pathological brain images.

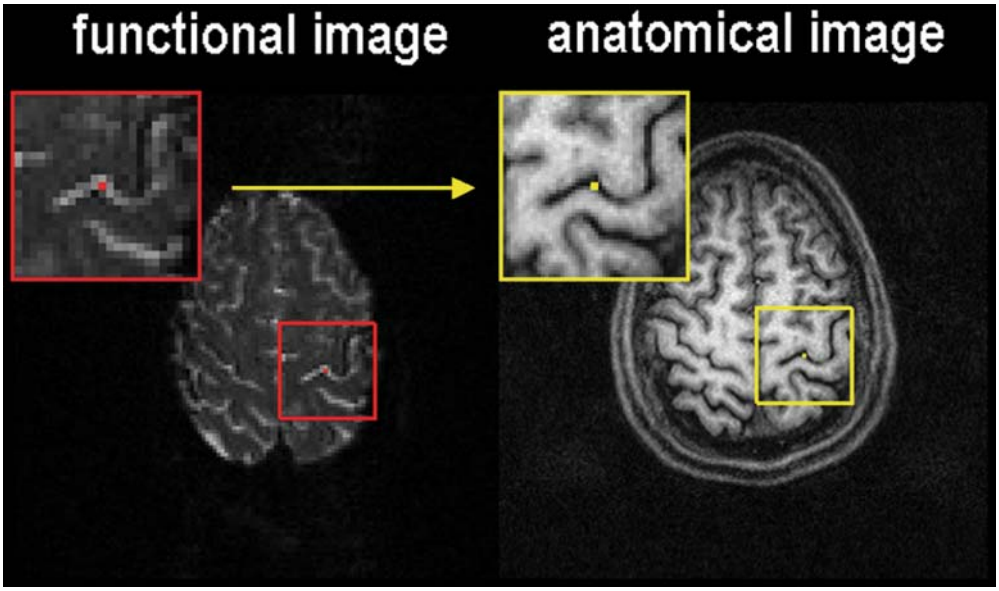

Fig. 1 Example for the localization of a reference point. Left: functional image with a freely selected reference point (red) within the primarily activated structures of the central sulcus/primary motor cortex. Right: anatomical image with overlay of the reference point to the corresponding anatomical structure by an fMRI expert. (Both images from subject 1)

The EPI volumes were then co-registered to the undistorted anatomical images by linear transformations using the free programs vtkCISG [40] (Thomas Hartkens, Computational Imaging Science Group, King's College London, London, UK, http://www.image-registration.com/ or http://www-ipg.umds.ac.uk/cisg/vtk-software/), SPM2 (coregistration function, Wellcome Department of Imaging Neuroscience, Functional Imaging Laboratory, London, UK, http://www.fil.ion.ucl.ac.uk/spm/software/spm2) and FSL [41] (FLIRT tool; Mark Jenkinson, FMRIB Software Library (FSL), Analysis Group, FMRIB, Oxford, UK, http://www.fmrib.ox.ac.uk/fsl/flirt). With SPM2, rigid coregistration (i.e., six parameters—three translation and three rotation parameters) was performed as implemented in the SPM2 coregistration menu. With vtkCISG and FLIRT the coregistration was done using affine (i.e., 12 parameters—three translation, three rotation, three scaling and three shearing parameters) transformations. The automatic coregistration was carried out using a masked anatomy with manually removed skull bone (see Fig. 2), since a recent study [42] revealed that this "skull-stripping" clearly improves the accuracy of the coregistration programs. We used the free program MRIcro (Chris Rorden, University of Nottingham, Great Britain, http://www.

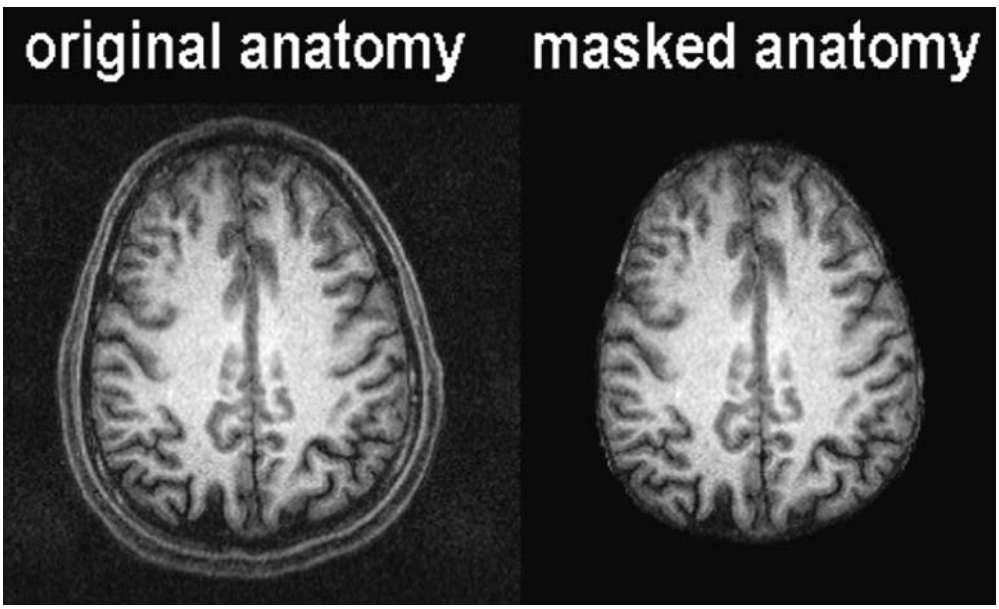

Fig. 2 Procedure of masking of anatomical images. Left: original, unmasked anatomical image. Right: anatomical image with masked (manually removed) skull bone. (Both images from subject 1)

psychology.nottingham.ac.uk/staff/cr1/mricro.html) for the masking process. While the FMRIB Software Library (FSL) also contains an automatic solution for extracting the brain (BET—brain extraction tool), which is also integrated in MRIcro, we chose manual masking to ensure comparable cortex delineation for every single case, independent of noise fluctuations in the data.

With all three programs, normalized mutual information was used as a similarity measure. (AIR was only used to remove head movement artifacts during the realignment process, but not for coregistration, since it does not support mutual information based cost functions.) From each coregistration setting a parameter set (containing 12 parameters with affine or 6 parameters with rigid transformation) was obtained. To compute the localization of the reference point in the anatomical volumes after coregistration, artificial volumes with the same spatial parameters as the EPI volumes, but containing only the selected reference point (all other voxels set to zero), were created and transformed using the obtained parameter sets. The transformed reference point volumes were then overlaid on the anatomical images to show the position of the reference point in relation to undistorted neuroanatomical structures. Due to interpolation during the transformation process, the reference point was blurred. Its correct localization was therefore calculated as the weighted mean of all non-zero voxels in the transformed volume.

Table 1 Evaluation of deviations between experts and programs for healthy subjects and patients

Healthy subjects			
Subject	Age	Sex	3D distance (mm) between *median* expert localization and *median* automatic localization
S1	24	m	2.4
S2	26	m	Max. 6.1
S3	19	m	4.1
S4	25	f	4.6
S5	18	m	2.7
S6	25	m	5.5
S7	31	m	4.0
S8	27	f	5.3
S9	26	m	5.1
S10	18	f	Min. 1.6
Mean±SD			4.2±1.5
Patients			
Patient	Age	Sex	3D distance (mm) between *median* expert localization and *median* automatic localization
P1	37	m	6.5
P2	55	f	5.8
P3	43	f	5.2
P4	48	m	13.2
P5	72	f	Min. 3.3
P6	30	m	7.0
P7	38	f	4.5
P8	33	f	6.3
P9	44	m	Max. 14.6
P10	10	f	3.9
Mean±SD			7.0±3.8

Note: 3D distances (mm) between median fMRI expert reference point localization and median automated reference point localization on the anatomical images are shown. The minimum, respectively, maximum 3D distances are marked separately, and the mean and standard deviation (SD) of the 3D distances are given for both groups of patients and healthy subjects. The 3D distances are significantly larger for patients than for healthy subjects according to an unpaired t-test (P=0.040).

The coregistration procedure resulted in three different reference point localizations (one for each program) for each of the ten patients and ten healthy subjects. In addition three different reference point localizations resulted from the manual transferals of the three fMRI experts. To check the differences between human experts and software solutions, the median 3D localizations for human experts and programs and the 3D distances between these two median localizations were calculated and evaluated by an unpaired t-test (see Table 1, Figs. 3 and 4). In addition, the quality of the reference point localizations produced by experts and programs was evaluated by a qualitative visual rating of Fig. 3 (see Table 2).

As a next step, we investigated the inter-rater variability for the fMRI experts and the software solutions. For this, the reference point localization on the anatomical data was compared between each of the fMRI experts resulting in three distance values (3D distance of reference point localization of expert A vs. localization of expert B, expert A vs. expert C and expert B vs. expert C). The same procedure was repeated for the programs.

Kolmogorov-Smirnov tests were used to check for deviations from normal distribution. The maximum of the 3D distances between each of the three human experts, respectively, three programs (calculated separately for each of the 20 participants) was used as an indicator for the inter-rater variability (Table 3). While above the median was chosen to calculate a robust measure for the "agreement" between the localizations of the three experts and programs, here we chose the maximum to calculate the "disagreement" between the three localizations as a measure of maximum variability. This was done since in clinical applications the worst possible localization performance should be known. Since this approach includes evaluation of outliers, an additional analysis comprised only the minimum deviations between programs or experts. This allows evaluation of program-expert differences when only the best-performing techniques are used. Two mixed-measures analysis-of-variances (ANOVAs) were calculated to test the dependence of these values from the within-subject factor of "experts vs. programs" and the between-subject factor of "patients vs. healthy subjects."

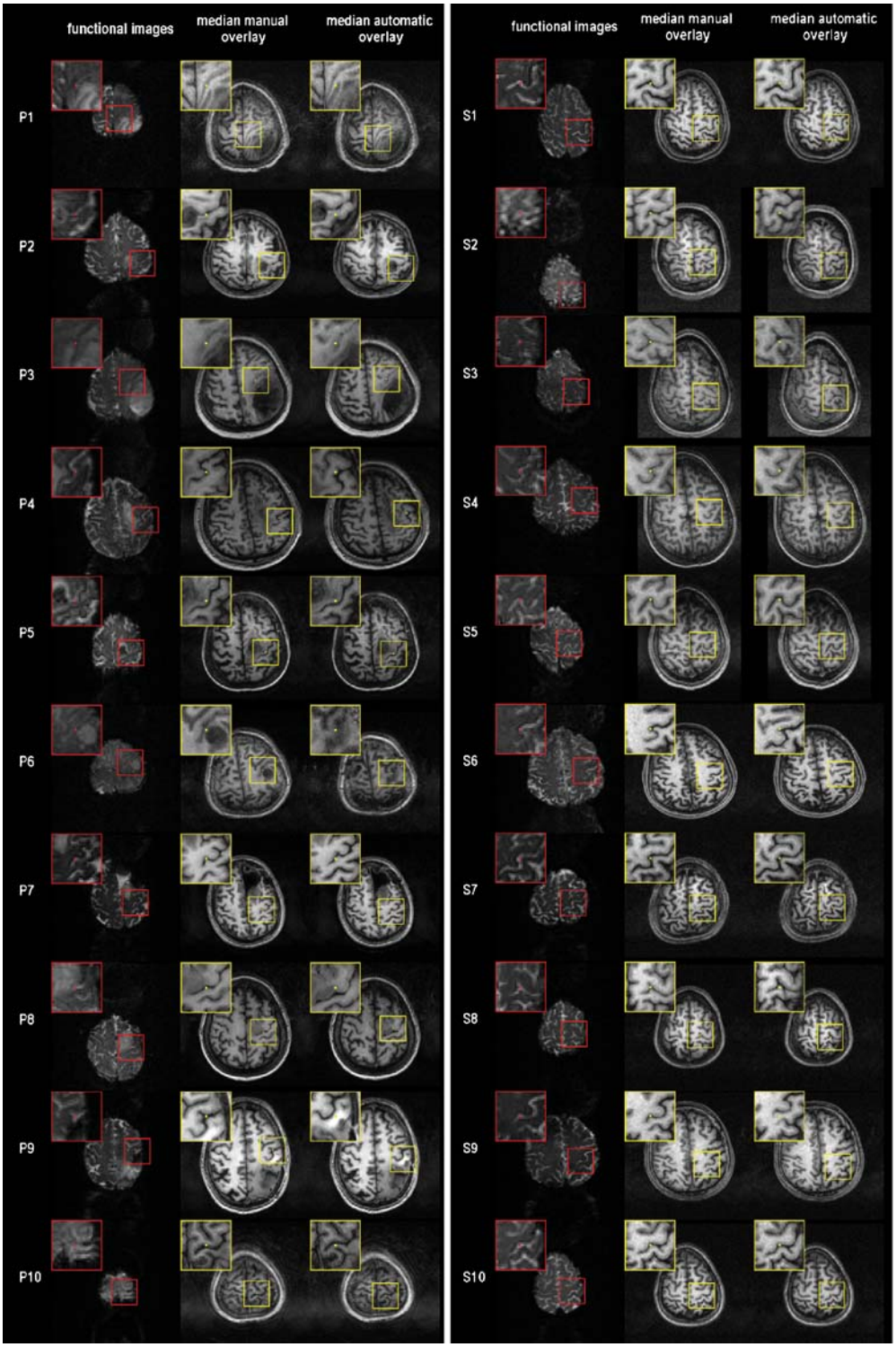

Fig. 3 Detailed results of reference point localizations with experts and programs. For each of the patients (P1–P10) and healthy subjects (S1–S10) three images are shown. Left: the functional data set with the selected reference point. Middle: the median position of the reference point in the anatomical data set according to the three fMRI expert raters. Right: the median position of the reference point in the anatomical data set according to the three automatic coregistration programs

Results

All statistical distributions used in this section were tested for significant deviations from normal distribution with Kolmogorov-Smirnov tests, which remained non-significant in all cases. Therefore, normal distribution was assumed. The median expert localizations and program localizations are shown together with the originally

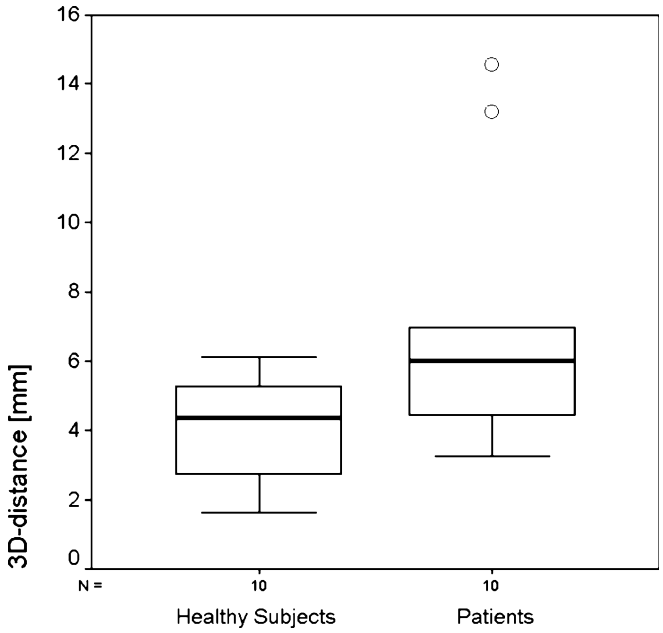

Fig. 4 Evaluation of deviations between experts and programs. 3D distances (mm) between the median reference point localizations of human experts and programs are shown for healthy subjects and patients. The boxplots show median (line across the box), inter-quartile distance (box: 25th to 75th percentile), largest/smallest value within one and a half box lengths outside box (whiskers), outliers (circles) of the distribution. Note that the deviations between experts and programs are significantly larger for the patient population (unpaired t-test: P=0.040)

Table 2 Evaluation of localization performance based on visual inspection of Fig. 3 for healthy subjects and patients

Healthy subjects			
Subject	Age	Sex	**Best localization by**
S1	24	m	Experts and programs
S2	26	m	Experts
S3	19	m	Experts and programs
S4	25	f	Experts
S5	18	m	Experts and programs
S6	25	m	Experts
S7	31	m	Experts and programs
S8	27	f	Experts
S9	26	m	Experts
S10	18	f	Experts and programs
Patients			
Patient	Age	Sex	**Best localization by**
P1	37	m	Experts
P2	55	f	Experts
P3	43	f	Experts
P4	48	m	Experts
P5	72	f	Experts and programs
P6	30	m	Experts
P7	38	f	Experts
P8	33	f	Experts
P9	44	m	Experts
P10	10	f	Experts

selected anatomical reference point of the functional datasets in Fig. 3 for all of the ten patients and ten healthy subjects. Table 1 shows the distances between the median localizations of the human experts and the programs. A clear difference was found between experts and software (mean 3D distance 5.6 mm over all patients and subjects). A qualitative visual analysis of the results shown in Fig. 3 is given in Table 2. The results of this evaluation are more or less self-evident and revealed that in 70% the expert's localization was superior to the software solutions. Within the patients group even 90% of the expert localizations were better.

When comparing patients and healthy subjects, the deviation between experts and software was significantly larger for patients than for healthy subjects according to an unpaired t-test (P=0.040; mean for healthy subjects: 4.2 mm; mean for patients: 7.0 mm, Fig. 4).

Concerning inter-rater variability, Table 3 shows the maxima of the 3D distances between the localizations of the human expert raters. Corresponding values were calculated for the programs. We took these maxima as indicators for the inter-rater variance and compared experts and programs by a mixed-measures ANOVA. Here, the within-subject factor "experts vs. programs" became significant (P=0.003), while the between-subject factor "patients vs. healthy subjects" (P=0.192) and the interactions between these two factors (P=0.669) remained non-significant. A subsequent evaluation of means (paired t-test: P=0.003; mean for programs: 13.8 mm; mean for experts: 3.6 mm) indicated that the inter-rater variability is significantly larger for the programs than for the experts (Fig. 5).

The analysis of the two patient data sets from the 1.5-T Philips system showed in one (out of six) automatic coregistration results a substantial difference between the Bruker and Philips data sets.

Discussion

This pilot study provides a first evaluation of whether the localization of motor activity on anatomical images may differ between software solutions and trained clinical fMRI experts. All analyses were restricted to the primary sensorimotor cortex since this structure plays an important role in clinical fMRI diagnostics. For the evaluation of localization variability, a functional reference point was chosen within the functional MRI data set at a characteristic location within the central sulcus/primary motor cortex of the functional images.

Table 3 Evaluation of inter-rater variability for experts and programs in healthy subjects and patients

3D distances between the three human experts			
Healthy subjects			
Subject	Age	Sex	Maximum 3D distance of expert localizations (mm)
S1	24	m	4.9
S2	26	m	Max. 6.4
S3	19	m	1.6
S4	25	f	2.9
S5	18	m	1.1
S6	25	m	1.3
S7	31	m	1.6
S8	27	f	Min. 0.9
S9	26	m	1.3
S10	18	f	2.2
Mean±SD			2.4±1.8
Patients			
Patient	Age	Sex	Maximum 3D distance of expert localizations (mm)
P1	37	m	7.8
P2	55	f	4.1
P3	43	f	3.6
P4	48	m	1.9
P5	72	f	Max. 11.2
P6	30	m	5.3
P7	38	f	Min. 0.9
P8	33	f	4.0
P9	44	m	1.9
P10	10	f	7.8
Mean±SD			4.8±3.2
3D distances between the three programs			
Healthy subjects			
Subject	Age	Sex	Maximum 3D distance of software localizations (mm)
S1	24	m	10.1
S2	26	m	12.9
S3	19	m	Max. 26.8
S4	25	f	6.5
S5	18	m	10.8
S6	25	m	Min. 3.8
S7	31	m	10.2
S8	27	f	4.2
S9	26	m	20.6
S10	18	f	6.7
Mean±SD			11.3±7.3
Patients			
Patient	Age	Sex	Maximum 3D distance of software localizations (mm)
P1	37	m	4.3
P2	55	f	39.6
P3	43	f	Max. 50.7
P4	48	m	11.4
P5	72	f	5.3
P6	30	m	13.8
P7	38	f	Min. 3.3
P8	33	f	5.7
P9	44	m	21.8
P10	10	f	7.4
Mean±SD			16.3±16.4

Note: The maximum 3D distance (mm) between the localizations of the three human experts (tables above) and the three computer programs (tables below) is given for every participant. The mean and standard deviation (SD) of the maxima are also shown for each group. According to a mixed-measures ANOVA (see "Results"), the inter-rater variability is larger for programs than for fMRI experts ($P=0.003$).

When comparing the median anatomical reference point localizations of the experts with those of the programs, a maximum deviation of 6.1 mm was found in healthy subjects and up to 14.6 mm deviation was found in patients (compare Table 1, Fig. 4). However, the worst program performance produced differences (from the median localization of the experts) of up to 45.6 mm in patients and 22.6 mm in healthy subjects. A statistical evaluation of the deviations between experts and software showed that the difference between patients and healthy subjects is significant, indicating that expert and software solutions differ more with patients. Due to good image contrast a qualitative visual evaluation of localization results was easily accomplished and more or less self-evident. All data are given in Fig. 3 and Table 2. Results show that expert localizations were better than program localizations in 70% of the subjects and 90% of the patients. This indicates that the investigated software solutions do have particular difficulties with pathological brains (compare, e.g., [43]), which partly lack morphological contrast and also represent a larger mean population age.

A further analysis concerned inter-rater consistency. It was significantly lower for software solutions than for fMRI experts (Table 3, Fig. 5). A visual inspection of the coregistration results (compare also Table 3) revealed indeed that the program FLIRT produced outliers in two patients and two healthy subjects. A comparable behavior was not found for the fMRI experts.

What are the consequences of these findings for clinical fMRI? As indicated by Fig. 3, automatic registration errors in primary sensorimotor cortex may in some cases mistake the post central sulcus for the central sulcus (P1; S2) or shift the central sulcus to precentral areas (P8). The latter situation may be particularly dangerous, since active primary motor cortex tissue might here erroneously be designated as primary sensory cortex.

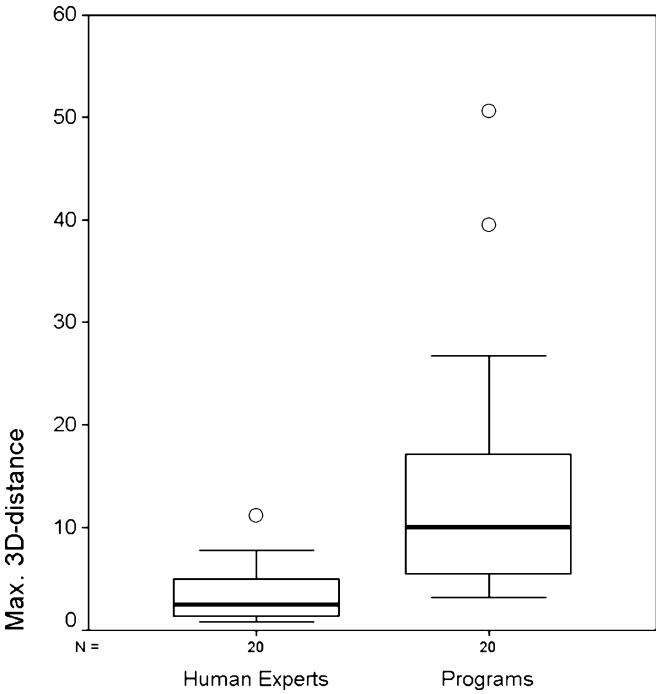

Fig. 5 Evaluation of inter-rater variability for experts and programs. Maximum 3D distances between the reference point localizations generated by human experts are shown on the left for all 20 participants. The boxplots show median (line across the box), interquartile distance (box: 25th to 75th percentile), largest/smallest value within one and a half box lengths outside box (whiskers), and outliers (circles) of the distribution. For programs the same is shown on the right. Inter-rater variability is larger for programs than for human experts (paired t-test: P=0.003)

The reasons for insufficient automatic coregistration results may be large distortions and/or ghost artifacts in the functional images, or a bad signal-to-noise ratio of the functional and/or anatomical images. For a qualitative check of a possible influence of anatomical image structure, two anatomical patient data sets additionally recorded on a 1.5-T Philips system (Philips Medical Systems, Gyroscan Intera) were also analyzed. In one of six software comparisons coregistration results were indeed substantially different between Bruker and Philips data sets. This result indicates that optimized image quality might reduce the localization problems of the software solutions. However, in clinical practice, valid results are required for every given hardware environment.

The amount of non-linearity of EPI image distortions may be another important factor for inferior software performance, since linear coregistration techniques are naturally limited here. Because non-linear registration is still not widely used in clinical environments and possible benefits are not clear, this work concentrated on the validation of linear coregistration.

For automatic coregistration we used only masked anatomical images where the skull bone was removed manually, because a recent study [42] showed that distracting structures can lead to huge coregistration errors. In contrast to normal subjects, where sulci and gyri are usually clearly distinguishable when good fMRI quality is provided, in patients morphological reference structures are often highly reduced (compare Fig. 3). Accordingly, the performance of the coregistration programs used in this study was significantly worse in the patients group (compare Tables 1 and 2, Figs. 3 and 4).

Various techniques exist that try to solve the problem of EPI image distortion in fMRI. Optimized shimming can reduce the magnetic field inhomogeneities to some extent. A very simple approach is to overlay the distorted EPI images directly on undistorted anatomy without any further effort [10–12]. In this study, the most commonly used technique was investigated: coregistration of the distorted EPI images with undistorted anatomical images (compare [20, 28, 29, 35] for basic and [31–34, 44] for clinical research). While early papers often used a contour fit approach [23–26], recent publications mostly apply volume-based approaches and maximization of (normalized) mutual information [20, 27, 28, 31, 32, 44, 45]. Concerning possible improvements of automatic coregistration, non-linear registration techniques may be advantageous in largely non-linearly distorted data sets. However, these methods still suffer from some drawbacks like poor robustness (especially with brain pathologies), difficult validation and long computation time [29, 43, 46].

Another sophisticated approach is the recording of B0 field maps, which are subsequently used for undistortion of the functional EPI images [18–22]. This technique currently is under increasing research; however, detailed quantifications of the residual error of B0 techniques are still missing. In a study by Hutton et al. [20], all B0 distortion correction methods that were analyzed improved the coregistration between functional and anatomical images, but none of the B0 methods did so for all of the data sets. This restriction is especially important in a clinical setting were functional localizations must be valid for every single patient. Up to now, no clinical data exist for B0 mapping results.

In summary, our data show that the validity and consistency of fMRI motor localizations on anatomical images is better with fMRI experts than with the tested coregistration programs and that this is particularly true for pathological brains. Of course, the results are directly linked to the hardware environment and technical parameters as applied in this pilot study. However, valid clinical fMRI localizations need to be possible with every local hardware situation, and due to considerable mislocalizations in some of our patients, we conclude that automatic coregistration techniques should be evaluated carefully, especially in case of clinical application. With no doubt, such software may be useful during the preparation of clinical or non-clinical reports, but detailed control by experienced clinical fMRI professionals seems recommendable [1, 2, 36, 37, 47–49]. Future research should extend evaluations of coregistration

results also to more critical brain areas (inferior frontal or temporal slices) and give special attention to recently developed methodology (non-linear registration techniques; B0 mapping) not yet in clinical use.

Acknowledgments This study was supported by the Austrian Science Fund FWF (P15102). We want to acknowledge important general support by Prof. Lueder Deecke, Department of Clinical Neurology, Medical University of Vienna, Head of the Ludwig Boltzmann Institute for Functional Brain Topography.

References

1. Beisteiner R (2006) Funktionelle Magnetresonanztomographie. In: Lehrner J, Pusswald G, Fertl E, Kryspin-Exner I, Strubreither W (eds) Klinische Neuropsychologie. Springer, Wien New York, pp 239–252
2. Beisteiner R, Barth M (2005) Probleme und Lösungsmöglichkeiten bei Patientenuntersuchungen mit funktioneller Magnetresonanztomographie (fMRT). In: Walter H (ed) Funktionelle Bildgebung in Psychiatrie und Psychotherapie–Methodische Grundlagen und Klinische Anwendungen. Schattauer, Stuttgart, pp 74–88
3. Vlieger E, Majoie C, Leenstra S et al (2004) Functional magnetic resonance imaging for neurosurgical planning in neurooncology. Eur Radiol 14:1143–1153. DOI 10.1007/s003300042328-y
4. Majos A, Tybor K, Stefañczyk L et al (2005) Cortical mapping by functional magnetic resonance imaging in patients with brain tumors. Eur Radiol 15:1148–1158. DOI 10.1007/s00330-004-2565-0
5. Hesselmann V, Maarouf M, Hunsche S et al (2006) Functional MRI for immediate monitoring stereotactic thalamotomy in a patient with essential tremor. Eur Radiol. DOI 10.1007/s00330-006-0211-8
6. Neugroschl C, Denolin V, Schuind F et al (2005) Functional MRI activation of somatosensory and motor cortices in a hand-grafted patient with early clinical sensorimotor recovery. Eur Radiol 15:1806–1814. DOI 10.1007/s00330-005-2763-4
7. Yetkin FZ, Rosenberg RN, Weiner MF et al (2006) FMRI of working memory in patients with mild cognitive impairment and probable Alzheimer's disease. Eur Radiol 16:193–206. DOI 10.1007/s00330-005-2794-x
8. Mansfield P (1977) Multi-planar image formation using NMR spin echoes. J Phys C 10:L55–L58. DOI 10.1088/0022-3719/10/3/004
9. Beisteiner R, Windischberger C, Lanzenberger R et al (2001) Finger somatotopy in human motor cortex. NeuroImage 13:1016–1026. DOI 10.1006/nimg.2000.0737
10. Kamada K, Houkin K, Takeuchi F et al (2003) Visualization of the eloquent motor system by integration of MEG, functional, and anisotropic diffusion-weighted MRI in functional neuronavigation. Surg Neurol 59:352–361; discussion 361–352. DOI 10.1016/S0090-3019(03)00018-1
11. Sabbah P, Foehrenbach H, Dutertre G et al (2002) Multimodal anatomic, functional, and metabolic brain imaging for tumor resection. Clin Imaging 26:6–12. DOI 10.1016/S0899-7071(01)00313-8
12. Braun V, Dempf S, Tomczak R et al (2001) Multimodal cranial neuronavigation: direct integration of functional magnetic resonance imaging and positron emission tomography data: technical note. Neurosurgery 48:1178–1181; discussion 1181–1172
13. Zhao Y, Anderson A, Gore J (2005) Computer simulation studies of the effects of dynamic shimming on susceptibility artifacts in EPI at high field. J Magn Reson 173:10–22. DOI 10.1016/j.jmr.2004.11.009
14. Cusack R, Russell B, Cox S et al (2005) An evaluation of the use of passive shimming to improve frontal sensitivity in fMRI. NeuroImage 24:82–91. DOI 10.1016/j.neuroimage.2004.08.029
15. Wilson J, Jenkinson M, de Araujo I et al (2002) Fast, fully automated global and local magnetic field optimization for fMRI of the human brain. NeuroImage 17:967–976. DOI 10.1016/S1053-8119(02)91172-9
16. Deichmann R, Gottfried J, Hutton C et al (2003) Optimized EPI for fMRI studies of the orbitofrontal cortex. NeuroImage 19:430–441. DOI 10.1016/S1053-8119(03)00073-9
17. Chen N, Wyrwicz A (2001) Optimized distortion correction technique for echo planar imaging. Magn Reson Med 45:525–528. DOI 10.1002/1522-2594(200103)45:3<525::AID-MRM1070>3.0.CO;2-S
18. Windischberger C, Robinson S, Rauscher A et al (2004) Robust field map generation using a triple-echo acquisition. J Magn Reson Imaging 20:730–734. DOI 10.1002/jmri.20158
19. Cusack R, Brett M, Osswald K (2003) An evaluation of the use of magnetic field maps to undistort echo-planar images. NeuroImage 18:127–142. DOI 10.1006/nimg.2002.1281
20. Hutton C, Bork A, Josephs O et al (2002) Image distortion correction in fMRI: A quantitative evaluation. NeuroImage 16:217–240. DOI 10.1006/nimg.2001.1054
21. Reber P, Wong E, Buxton R et al (1998) Correction of off resonance-related distortion in echo-planar imaging using EPI-based field maps. Magn Reson Med 39:328–330
22. Jezzard P, Balaban R (1995) Correction for geometric distortion in echo planar images from B0 field variations. Magn Reson Med 34:65–73
23. Ernst T, Speck O, Itti L et al (1999) Simultaneous correction for interscan patient motion and geometric distortions in echoplanar imaging. Magn Reson Med 42:201–205. DOI 10.1002/(SICI)1522-2594(199907)42:1<201::AID-MRM27>3.0.CO;2-Y
24. Nimsky C, Ganslandt O, Kober H et al (1999) Integration of functional magnetic resonance imaging supported by magnetoencephalography in functional neuronavigation. Neurosurgery 44:1249–1255; discussion 1255–1246
25. Fahlbusch R, Ganslandt O, Nimsky C (2000) Intraoperative imaging with open magnetic resonance imaging and neuronavigation. Childs Nerv Syst 16:829–831. DOI 10.1007/s003810000344
26. Kober H, Nimsky C, Vieth J et al (2002) Co-registration of function and anatomy in frameless stereotaxy by contour fitting. Stereotact Funct Neurosurg 79:272–283
27. Wells WM, 3rd, Viola P, Atsumi H et al (1996) Multi-modal volume registration by maximization of mutual information. Med Image Anal 1:35–51. DOI 10.1016/S1361-8415(01)80004-9
28. Crum W, Hartkens T, Hill D (2004) Non-rigid image registration: Theory and practice. Br J Radiol 77:S140–S153. DOI 10.1259/bjr/25329214

29. Crum W, Griffin L, Hill D et al (2003) Zen and the art of medical image registration: Correspondence, homology, and quality. NeuroImage 20:1425–1437. DOI 10.1016/j.neuroimage.2003.07.014
30. Chui H, Win L, Schultz R et al (2003) A unified non-rigid feature registration method for brain mapping. Med Image Anal 7:113–130. DOI 10.1016/S1361-8415(02)00102-0
31. Jannin P, Morandi X, Fleig OJ et al (2002) Integration of sulcal and functional information for multimodal neuronavigation. J Neurosurg 96:713–723
32. Jannin P, Fleig O, Seigneuret E et al (2000) A data fusion environment for multimodal and multi-informational neuronavigation. Comput Aided Surg 5:1–10. DOI 10.1002/(SICI)1097-0150(2000)5:1<1::AID-IGS1>3.0.CO;2-4
33. Hunsche S, Sauner D, Treuer H et al (2004) Optimized distortion correction of epi-based statistical parametrical maps for stereotactic neurosurgery. Magn Reson Imaging 22:163–170. DOI http://dx.doi.org/10.1016/j.mri.2003.08.006
34. Rutten G, Ramsey N, Noordmans H et al (2003) Toward functional neuronavigation: implementation of functional magnetic resonance imaging data in a surgical guidance system for intraoperative identification of motor and language cortices. Technical note and illustrative case. Neurosurg Focus 15: E6
35. Yokoi T, Soma T, Shinohara H et al (2004) Accuracy and reproducibility of co-registration techniques based on mutual information and normalized mutual information for MRI and SPECT brain images. Ann Nucl Med 18:659–667
36. Wilkinson I, Romanowski C, Jellinek D et al (2003) Motor functional MRI for pre-operative and intraoperative neurosurgical guidance. Br J Radiol 76:98–103. DOI 10.1259/bjr/66817309
37. Gumprecht H, Ebel G, Auer D et al (2002) Neuronavigation and functional MRI for surgery in patients with lesion in eloquent brain areas. Minim Invasive Neurosurg 45:151–153. DOI 10.1055/s-2002-34341
38. Edward V, Windischberger C, Cunnington R et al (2000) Quantification of fMRI artifact reduction by a novel plaster cast head holder. Hum Brain Mapp 11:207–213. DOI 10.1002/1097-0193(200011)11:3<207::AID-HBM60>3.0.CO;2-J
39. Woods RP, Grafton ST, Holmes CJ et al (1998) Automated image registration: I. General methods and intrasubject, intramodality validation. J Comput Assist Tomogr 22:139–152
40. Hartkens T, Rueckert D, Schnabel J et al (2002) VTK CISG registration toolkit: An open source software package for affine and non-rigid registration of single- and multimodal 3D images. BVM2002. Springer, Leipzig. Available at: http://sunsite.informatik.rwth-aachen.de/Publications/CEUR-WS/Vol-56/185.pdf. (accessed May 30, 2005)
41. Smith SM, Jenkinson M, Woolrich MW et al (2004) Advances in functional and structural MR image analysis and implementation as FSL. NeuroImage 23:S208–S219. DOI 10.1016/j.neuroimage.2004.07.051
42. Gartus A, Geissler A, Foki T et al (2005) Automatic coregistration of functional and anatomical data: Validation of some software solutions. NeuroImage 26:S41
43. Hutton B, Braun M (2003) Software for image registration: algorithms, accuracy, efficacy. Semin Nucl Med 33:180–192. DOI http://dx.doi.org/10.1053/snuc.2003.127309
44. Yoo S, Talos I, Golby A et al (2004) Evaluating requirements for spatial resolution of fMRI for neurosurgical planning. Hum Brain Mapp 21:34–43. DOI 10.1002/hbm.10148
45. Studholme C, Hill D, Hawkes D (1999) An overlap invariant entropy measure of 3D medical image alignment. Pattern Recognition 32:71–86. DOI 10.1016/S0031-3203(98)00091-0
46. Brett M, Leff AP, Rorden C et al (2001) Spatial normalization of brain images with focal lesions using cost function masking. NeuroImage 14:486–500. DOI 10.1006/nimg.2001.0845
47. Beisteiner R, Lanzenberger R, Novak K et al (2000) Improvement of presurgical patient evalation by generation of functional magnetic resonance risk maps. Neurosci Lett 290:13–16. DOI 10.1016/S0304-3940(00)01303-3
48. Beisteiner R (2004) Indikationen, Probleme und Ergebnisse der funktionellen MRT im Kindesalter. Pädiatrische Praxis 64:285–298
49. Geissler A, Lanzenberger R, Barth M et al (2005) Influence of fMRI smoothing procedures on replicability of fine scale motor localization. NeuroImage 24:323–331. DOI 10.1016/j.neuroimage.2004.08.042